

Rapid, low-cost prediction of geomagnetic perturbations from real-time solar wind measurements

Daniel R. Weimer
Research Professor



Space Weather Workshop
The Meeting of Science, Research, Applications, Operations, and Users
April 8-11, 2014 • Boulder, CO

The banner for the Space Weather Workshop features a central image of Earth from space. To the left is a large, glowing orange sun. To the right is a collage of images related to space weather and its effects, including an airplane, a satellite, a power line, a aurora, and a person in a space suit. The text is white and bold, set against a dark background.

New prediction model developed with support from one (small) grant from NSF National Space Weather Program. Started in 2009.

Magnetometer data source and processing:

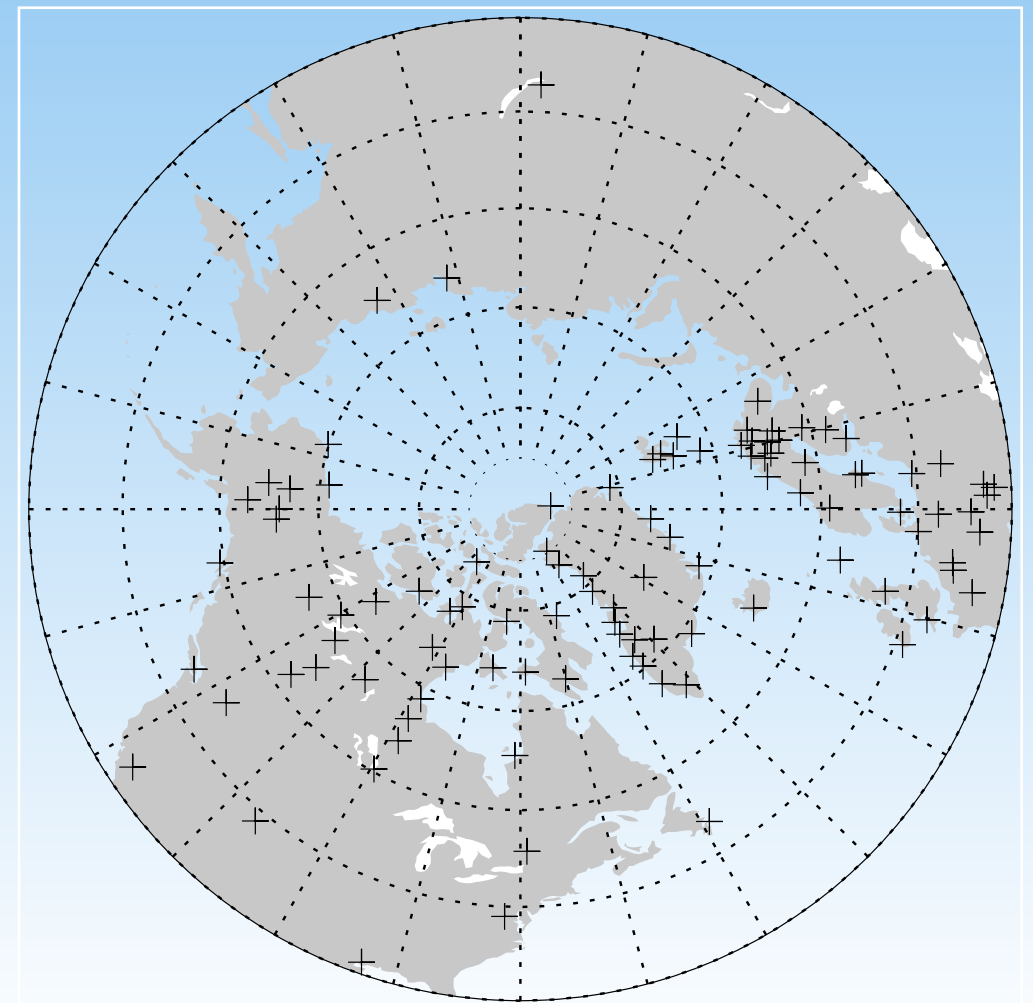
Weimer, D. R., C. R. Clauer, M. J. Engebretson, T. L. Hansen, H. Gleisner, I. Mann, and K. Yumoto (2010), Statistical maps of geomagnetic perturbations as a function of the interplanetary magnetic field, *J. Geophys. Res.*, *115*, A10320, 10.1029/2010JA015540.

Final model description:

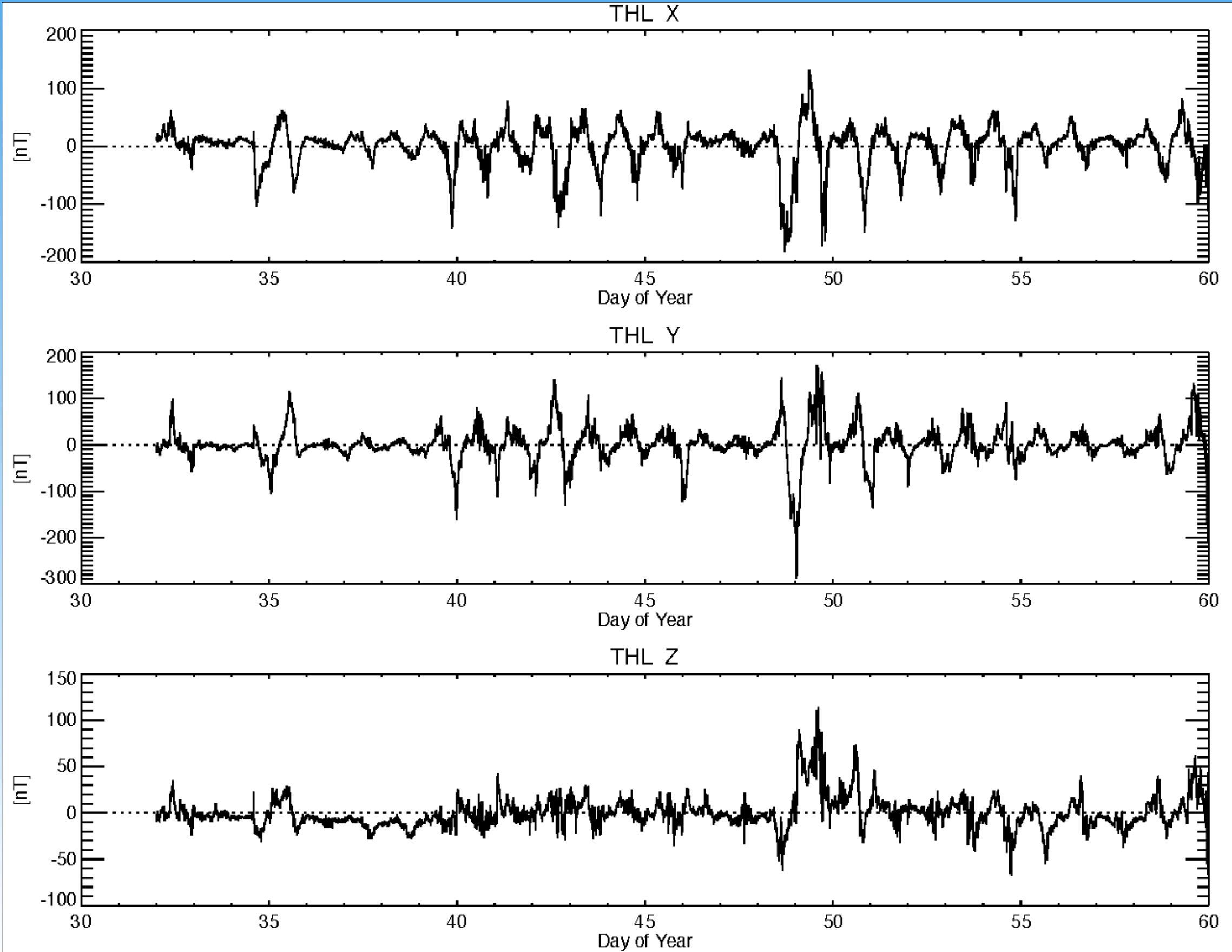
Weimer, D. R. (2013), An empirical model of ground-level geomagnetic perturbations, *Space Weather*, *11*, 107–120, doi:10.1002/swe.20030.

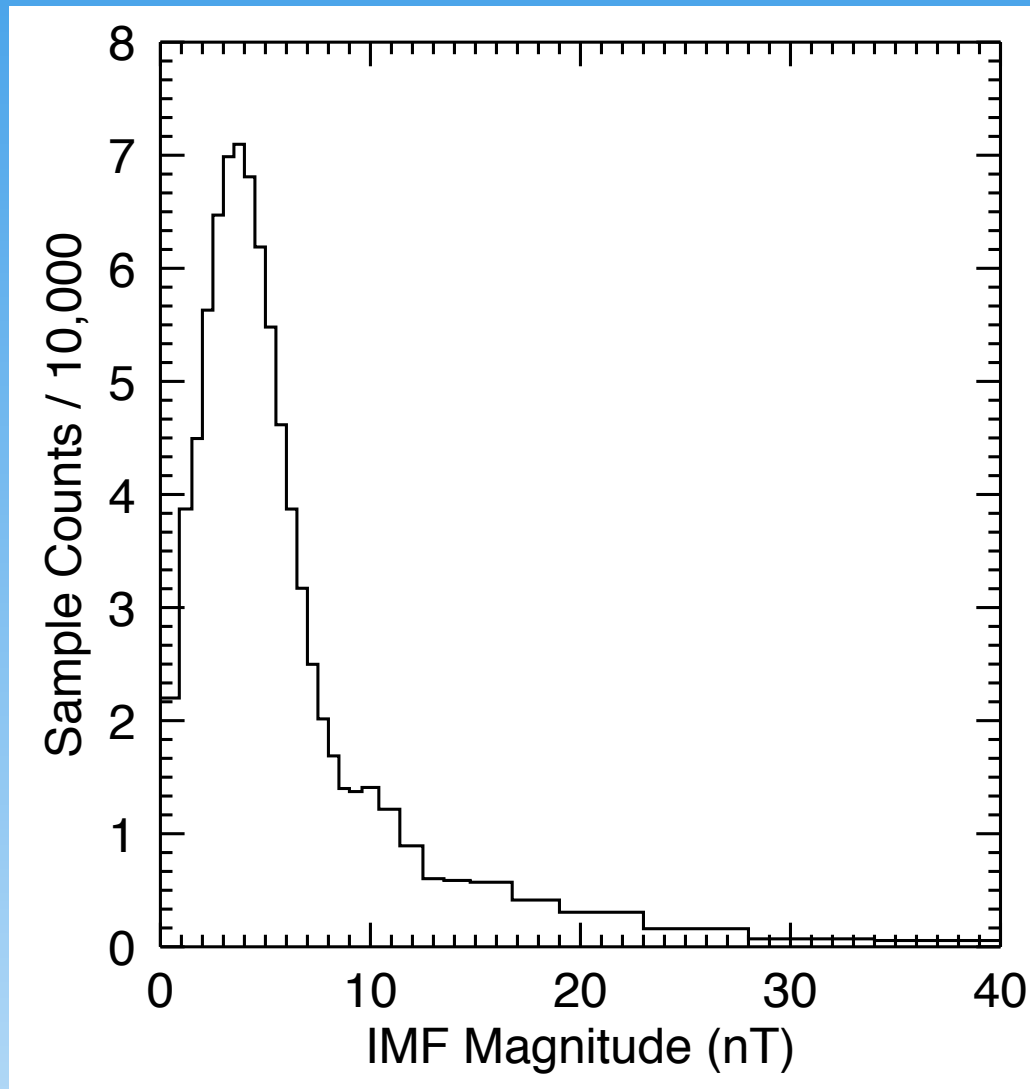
Uses data from >140 magnetometer stations in Northern hemisphere, over an 8-year period (1998-2005), solar wind velocity, IMF, and $F_{10.7}$.

Effects of conductivity variations and induced, underground currents are implicitly included.



Example of processed data, spanning one month ($\approx 13,000$ of these were examined for quality control)





The data are divided into 29 bins, sorted according to IMF magnitude. The width of each bin increased above 9 nT, yet there are few samples in the highest bins.

Model coefficients are derived using a least-error fit for each bin, including an over-lap of data from the adjacent bins.

Each vector component is fit separately, using spherical harmonics on a 90° cap, in corrected geomagnetic apex coordinates.

Only even l - m combinations of the Legendre polynomials are used.

To obtain a smooth response curve, the C_n coefficients are interpolated, given the IMF magnitude.

$$\Delta B_X(\Lambda, \varphi) = \sum_{l=0}^{31} \sum_{m=0}^{3<l} P_l^m(\cos \Lambda) (g_k^m \cos m\varphi + h_k^m \sin m\varphi)$$

$$g_k^m = c_0 + c_1 B_T + c_2 V_{SW} + c_3 t + c_4 \sqrt{F_{10.7}} +$$

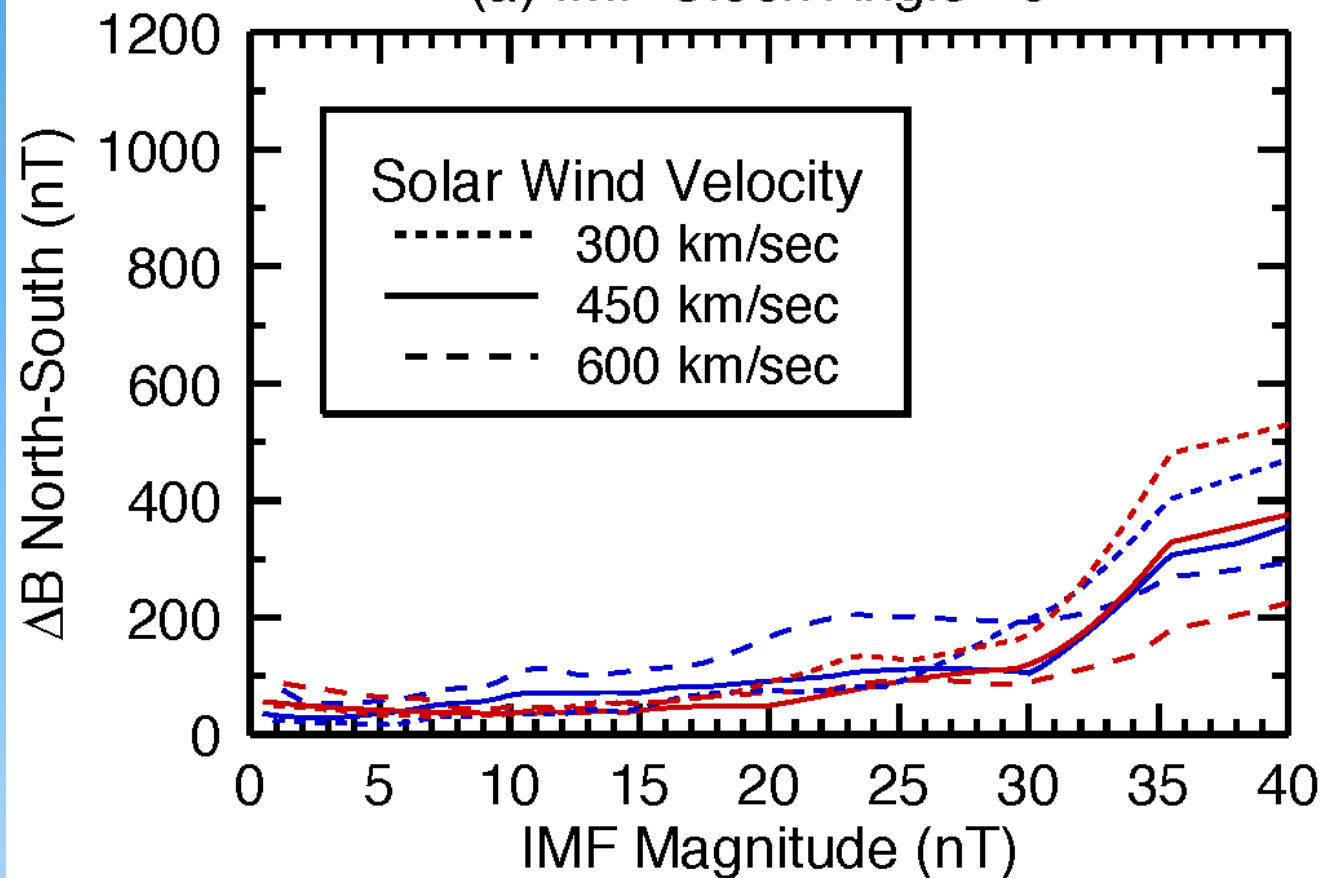
$$c_5 B_T \cos(\theta_c) + c_6 V_{SW} \cos(\theta_c) + c_7 t \cos(\theta_c) + c_8 \sqrt{F_{10.7}} \cos(\theta_c) +$$

$$c_9 B_T \sin(\theta_c) + c_{10} V_{SW} \sin(\theta_c) + c_{11} t \sin(\theta_c) + c_{12} \sqrt{F_{10.7}} \sin(\theta_c) +$$

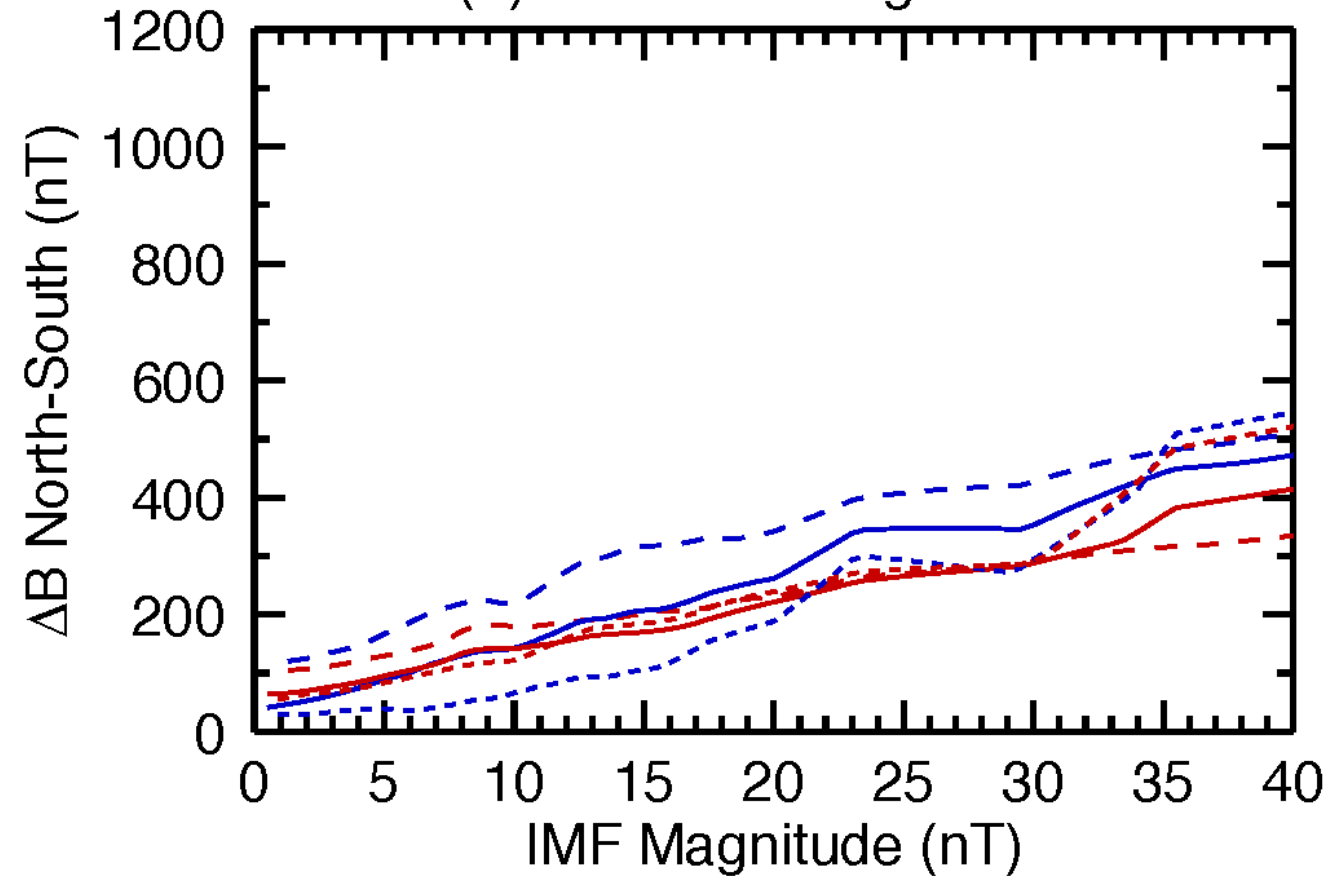
$$c_{13} B_T \cos(2\theta_c) + c_{14} V_{SW} \cos(2\theta_c) + c_{15} B_T \sin(2\theta_c) + c_{16} V_{SW} \cos(2\theta_c)$$

Saturation Curves—Minimum/Maximum Values vs. IMF

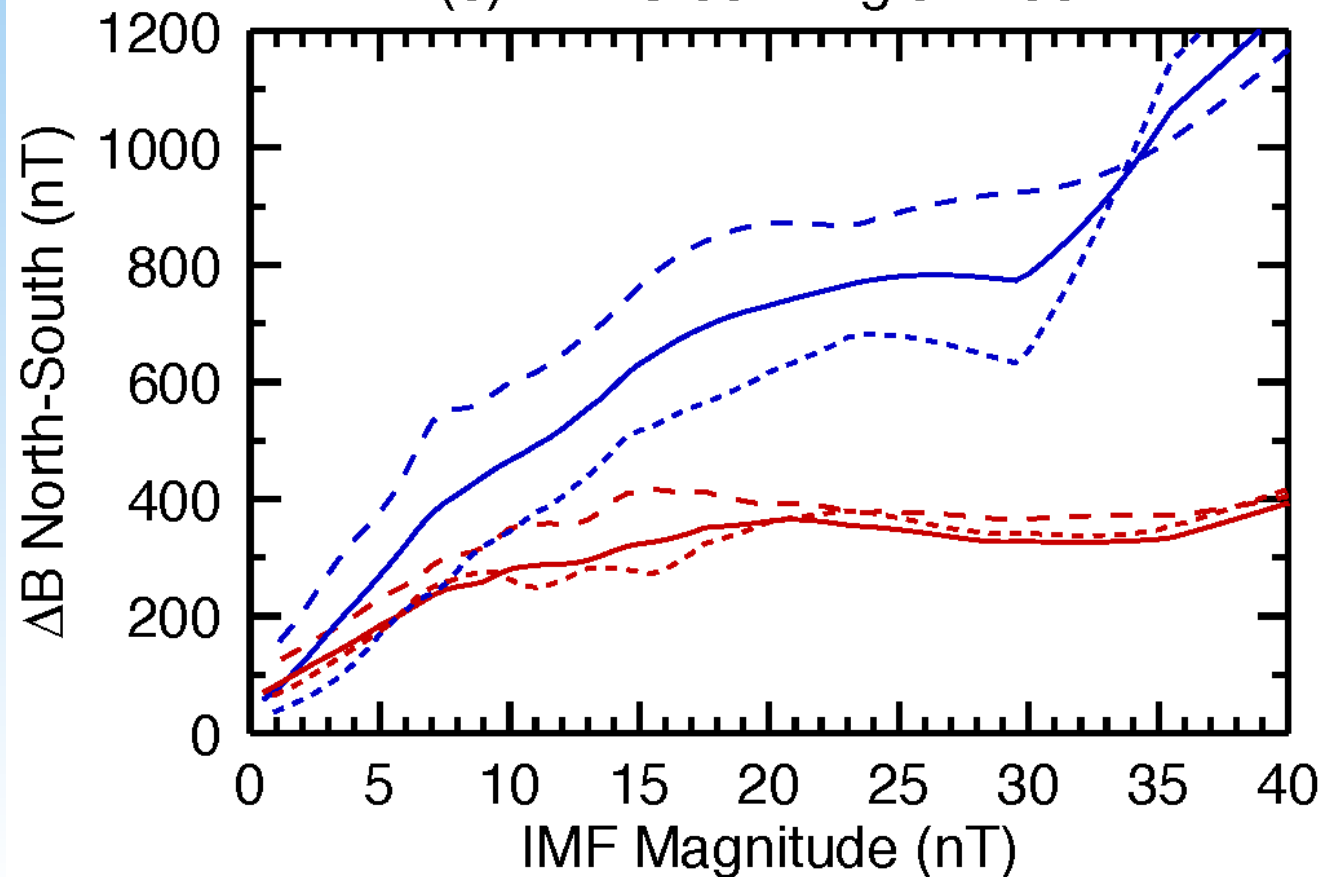
(a) IMF Clock Angle= 0°



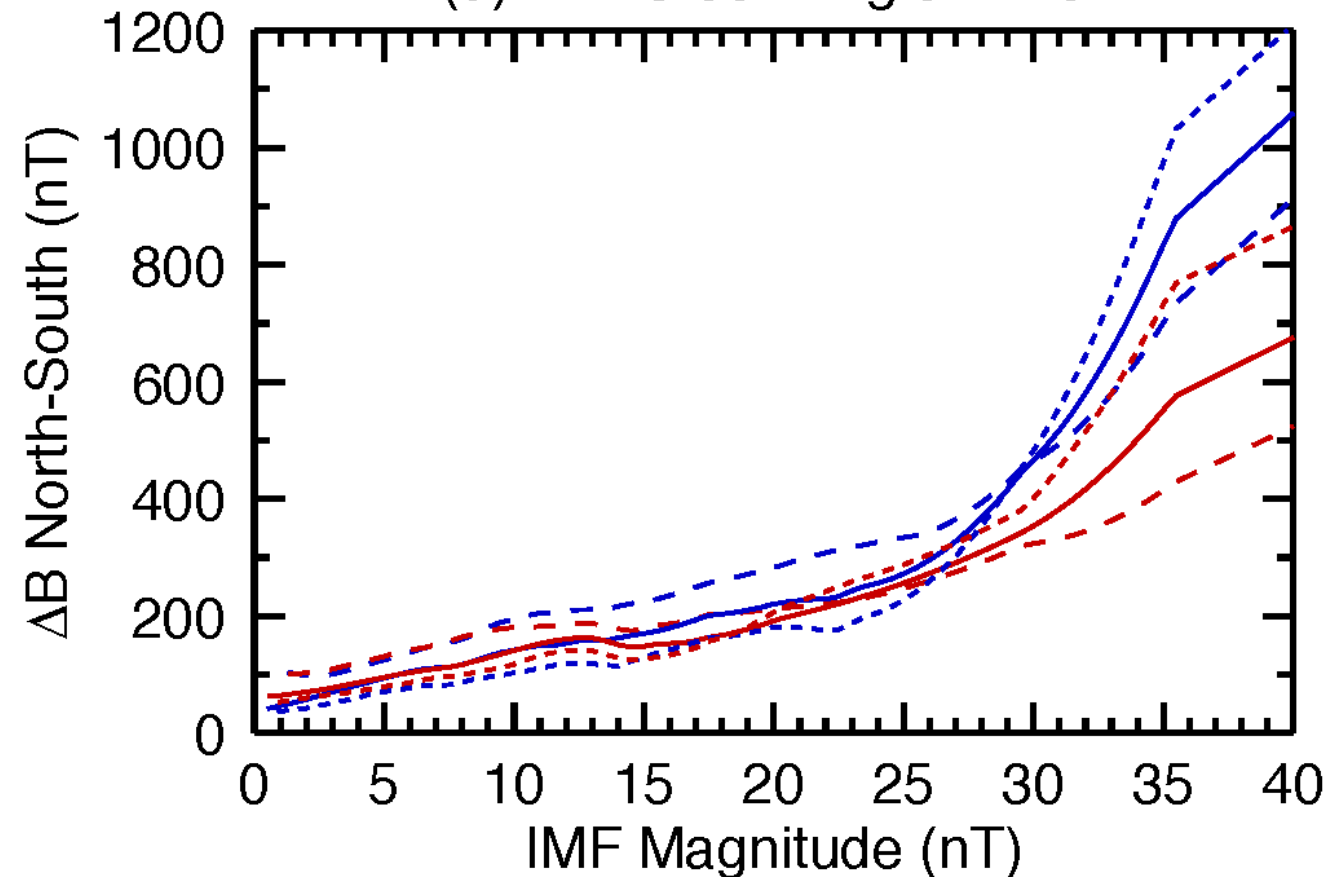
(b) IMF Clock Angle= 90°



(c) IMF Clock Angle= 180°

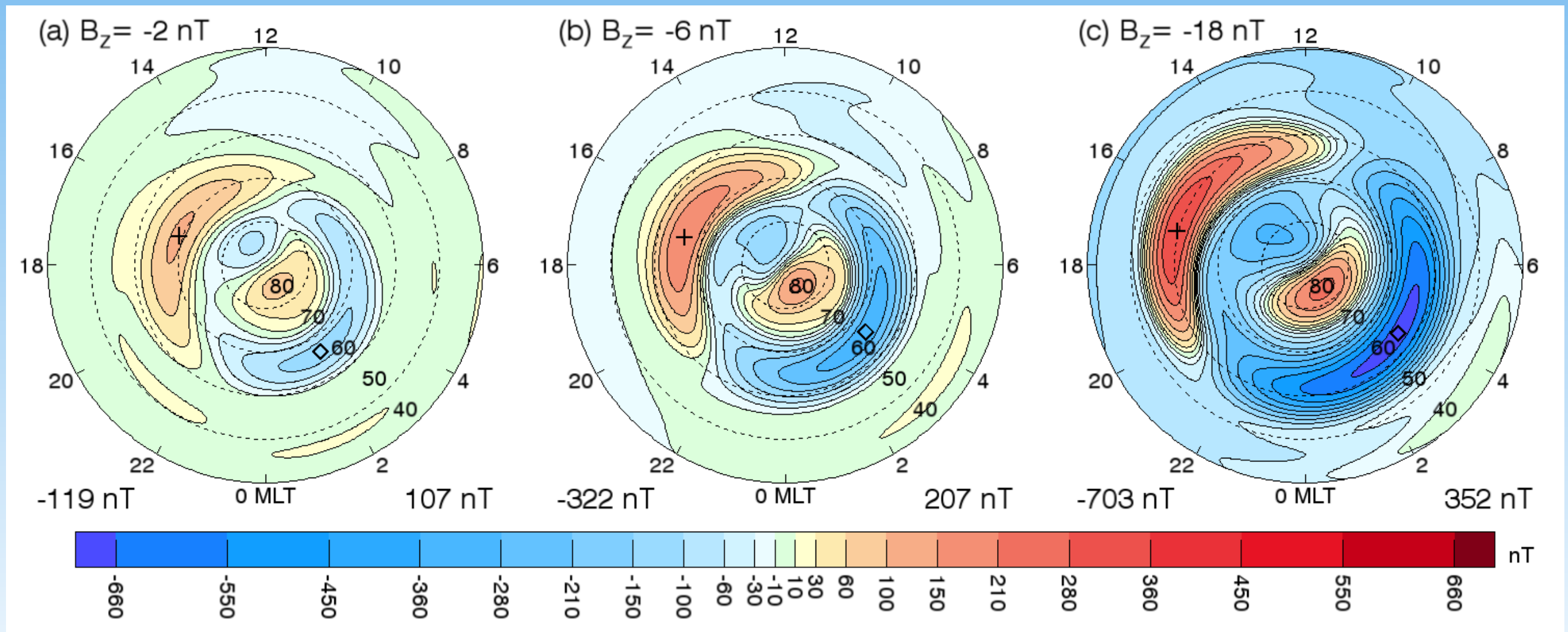


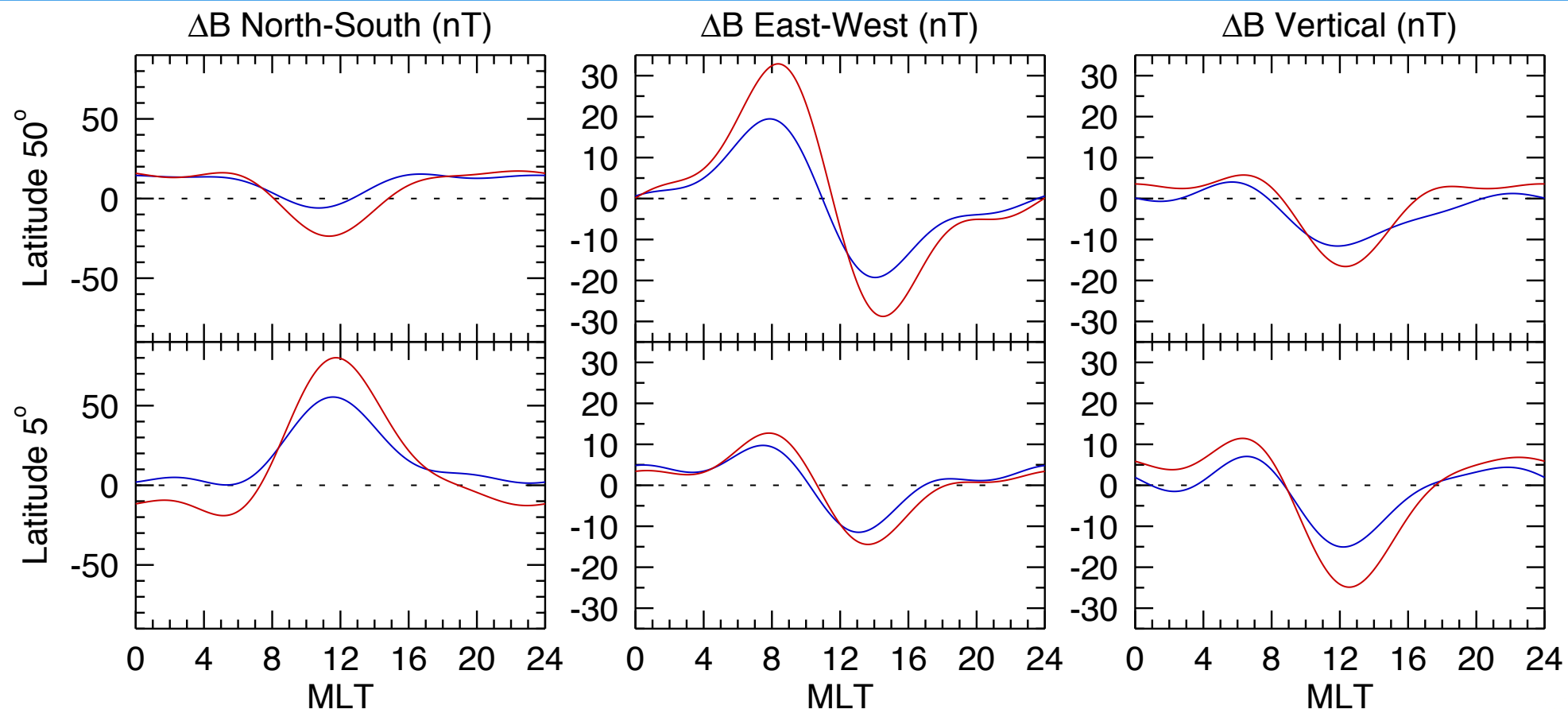
(d) IMF Clock Angle= 270°



Geomagnetic North-South component of ΔB , shown for IMF B_z values -2, -6, and -18 nT

The values become more negative at low latitudes, indicating that the effects of the ring current (Dst) are included in the statistical averages.





Effects of the Sq currents are shown in these graphs of ΔB -North (left), ΔB -East (middle), and ΔB -Vertical (right) versus MLT. These are shown for quiet conditions with a weakly northward IMF, at CGM apex latitudes of 5° and 50°. The red lines show the results with $F_{10.7} = 240$ sfu, and $F_{10.7} = 80$ sfu in the blue lines. Results compare very well with Figure 4-21. (Knecht, D. J., and B. M. Shuman (1985), *The geomagnetic field*, in *Handbook of geophysics and the space environment*, edited by A. S. Jursa, fourth ed., chap. 4, pp. 1-37, Air Force Geophysics Lab., Hanscom AFB, MA).

CHAPTER 4

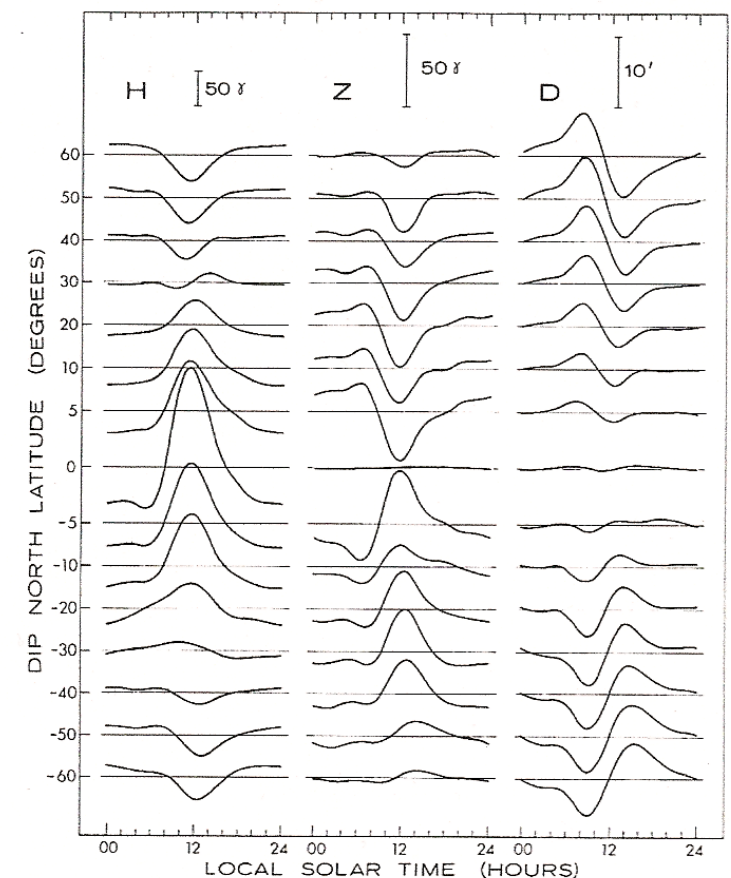
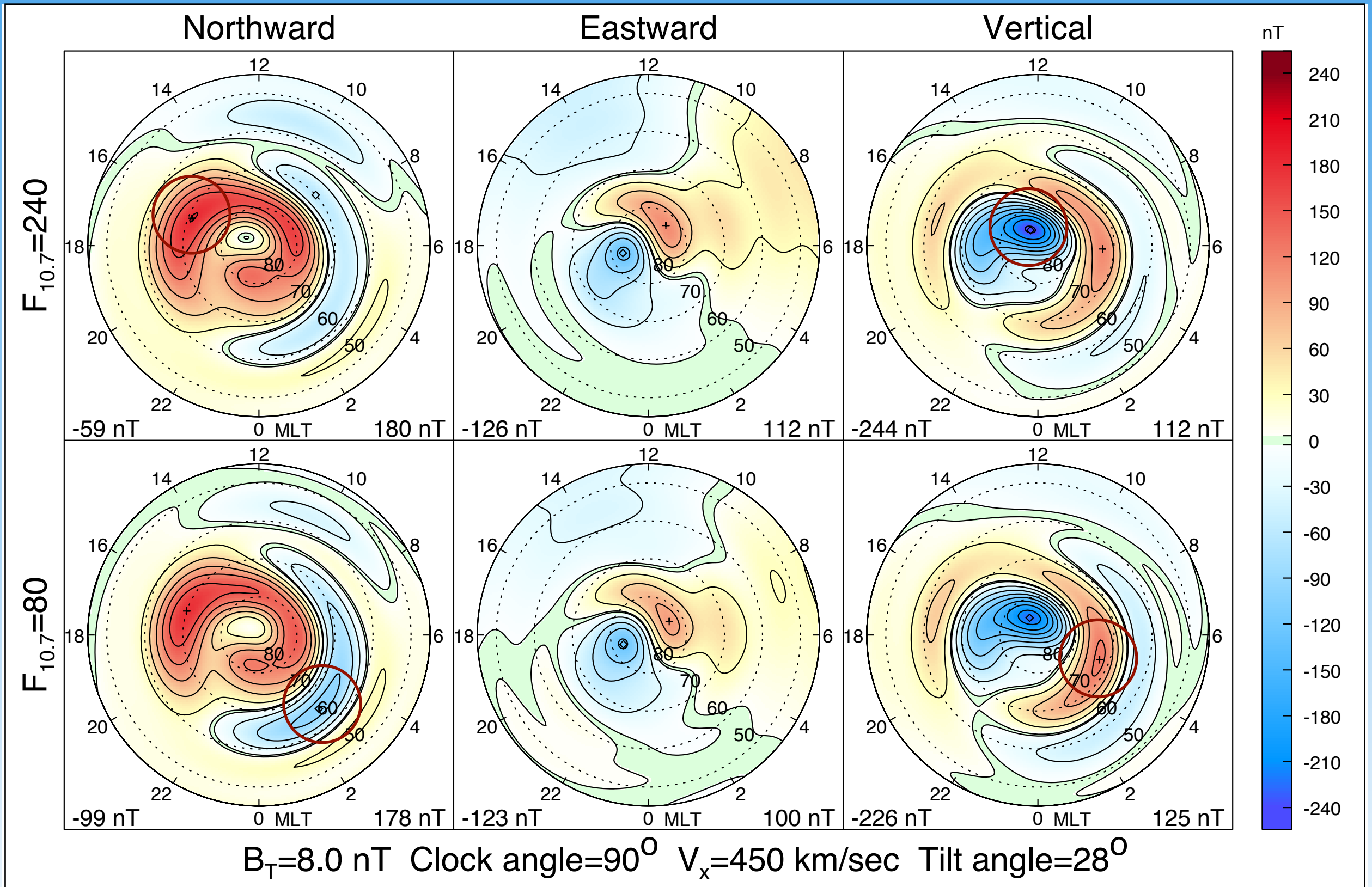


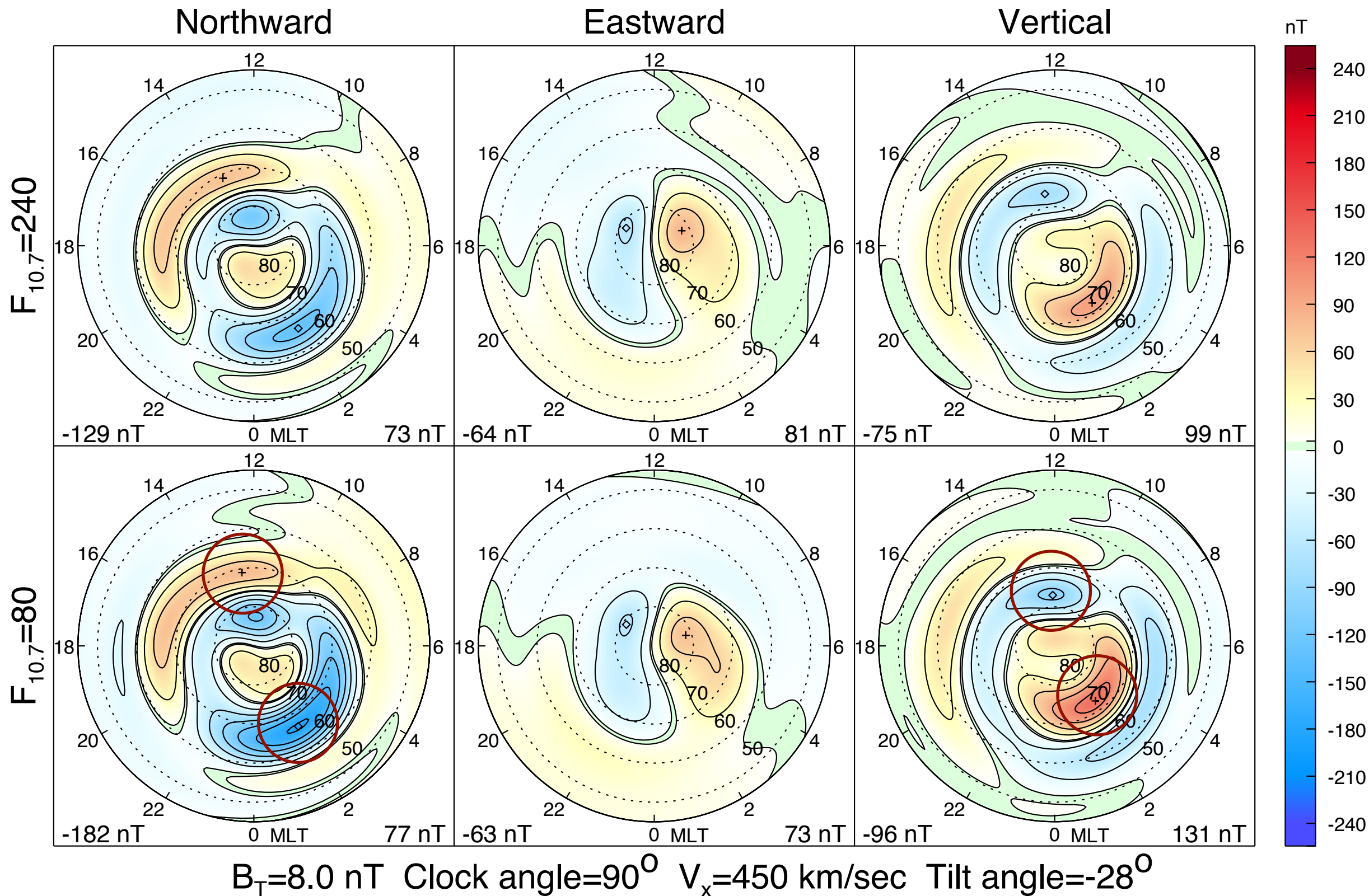
Figure 4-21. Worldwide average of the solar quiet variation near the equinoxes at solar maximum (March, April, September, and October, 1958) [after Matsushita, 1967].

+B_Y, Summer



Examples with low and high values of $F_{10.7}$. Results are not always as expected, as sometimes the smaller $F_{10.7}$ results in larger perturbations in some regions.

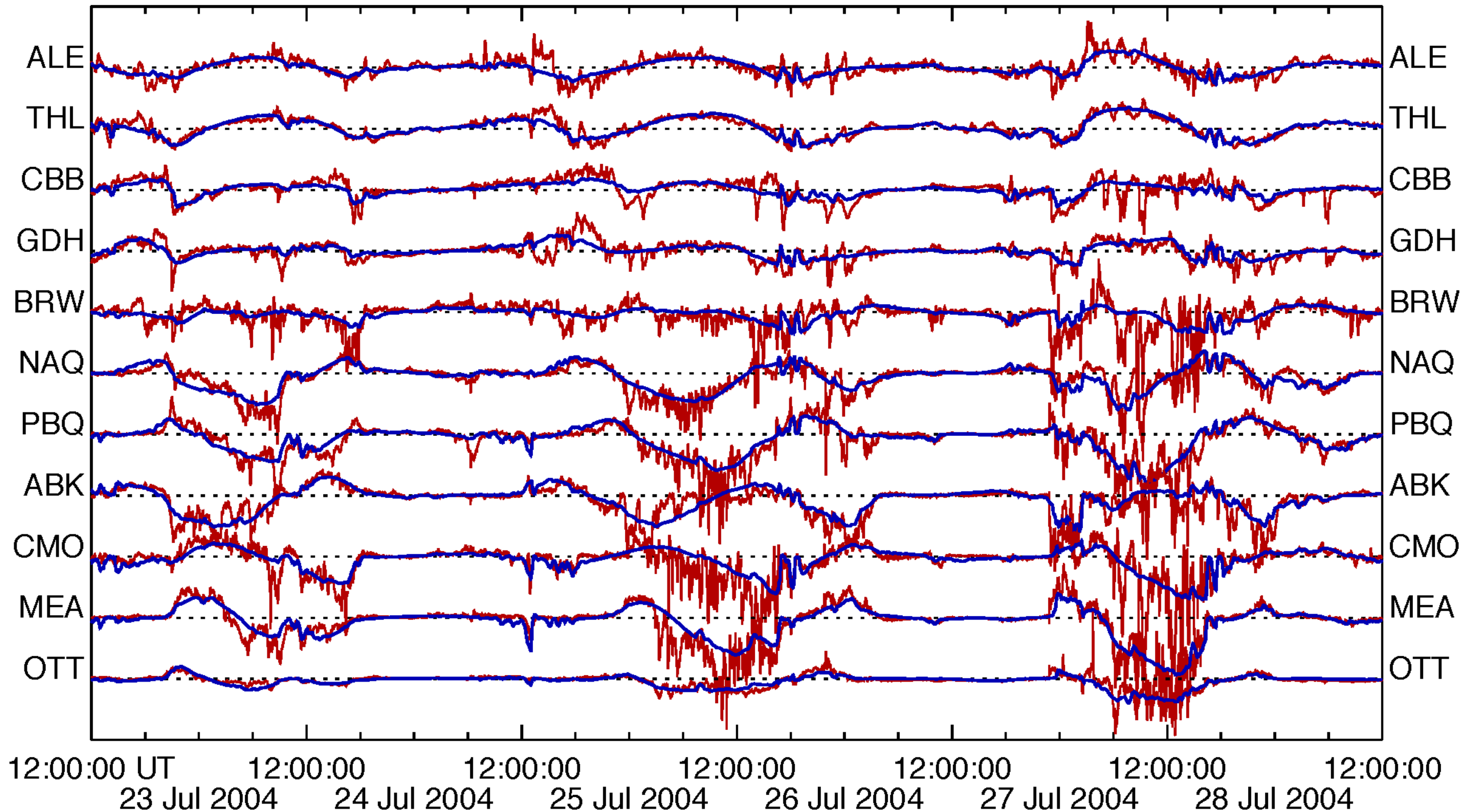
+B_y, Winter

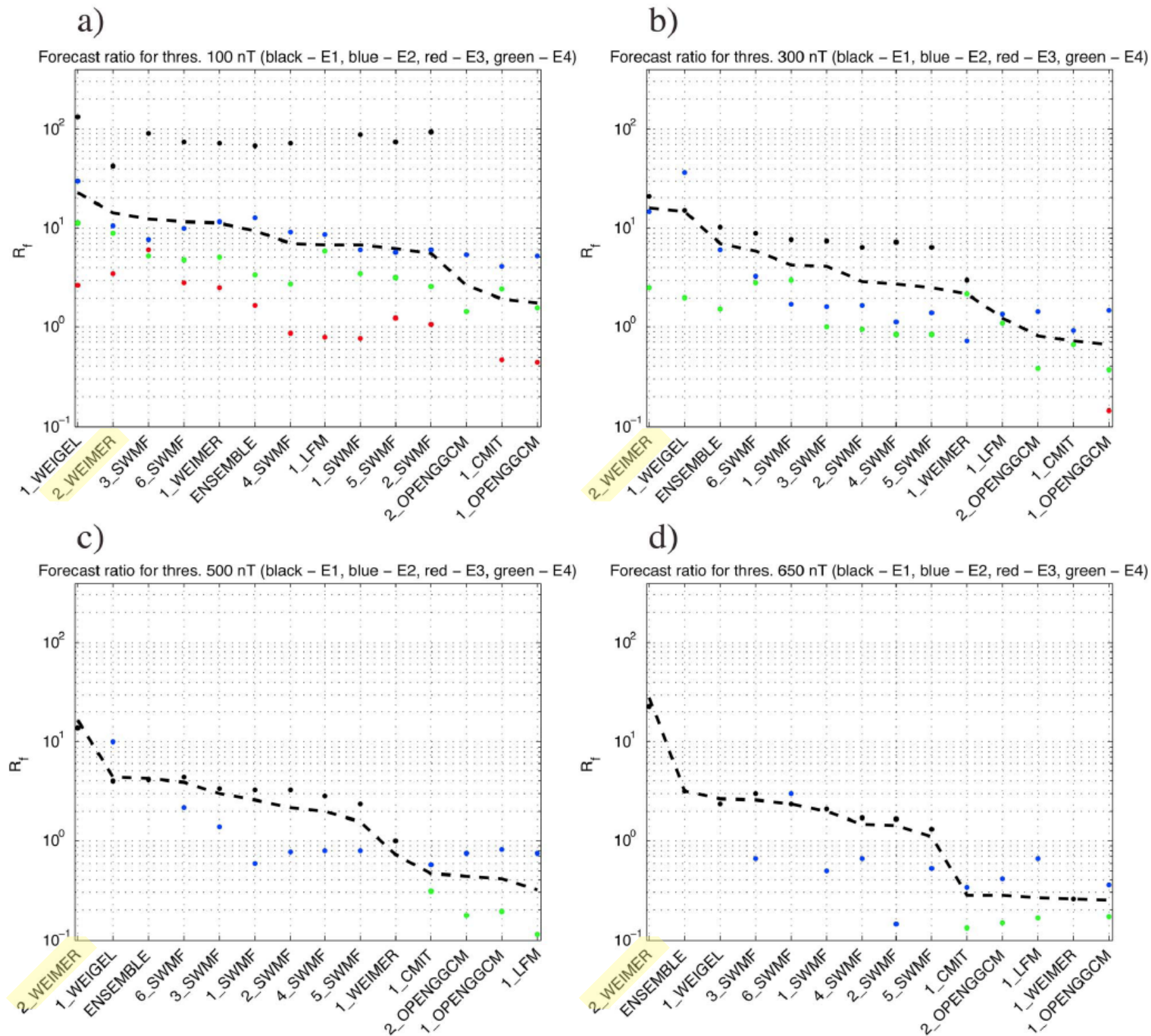


Examples with low and high values of $F_{10.7}$. Results are not always as expected, as sometimes the smaller $F_{10.7}$ results in larger perturbations in some regions.

The model does very well at prediction of ΔB levels; not so well on the superposed and random, higher frequency variations. Also does not include substorms.

ΔB North-South (X), 1200 nT between base lines





On first tests by NASA-CCMC that compared predictions with levels of ΔB , this model (earliest version) did better than others on most metrics.

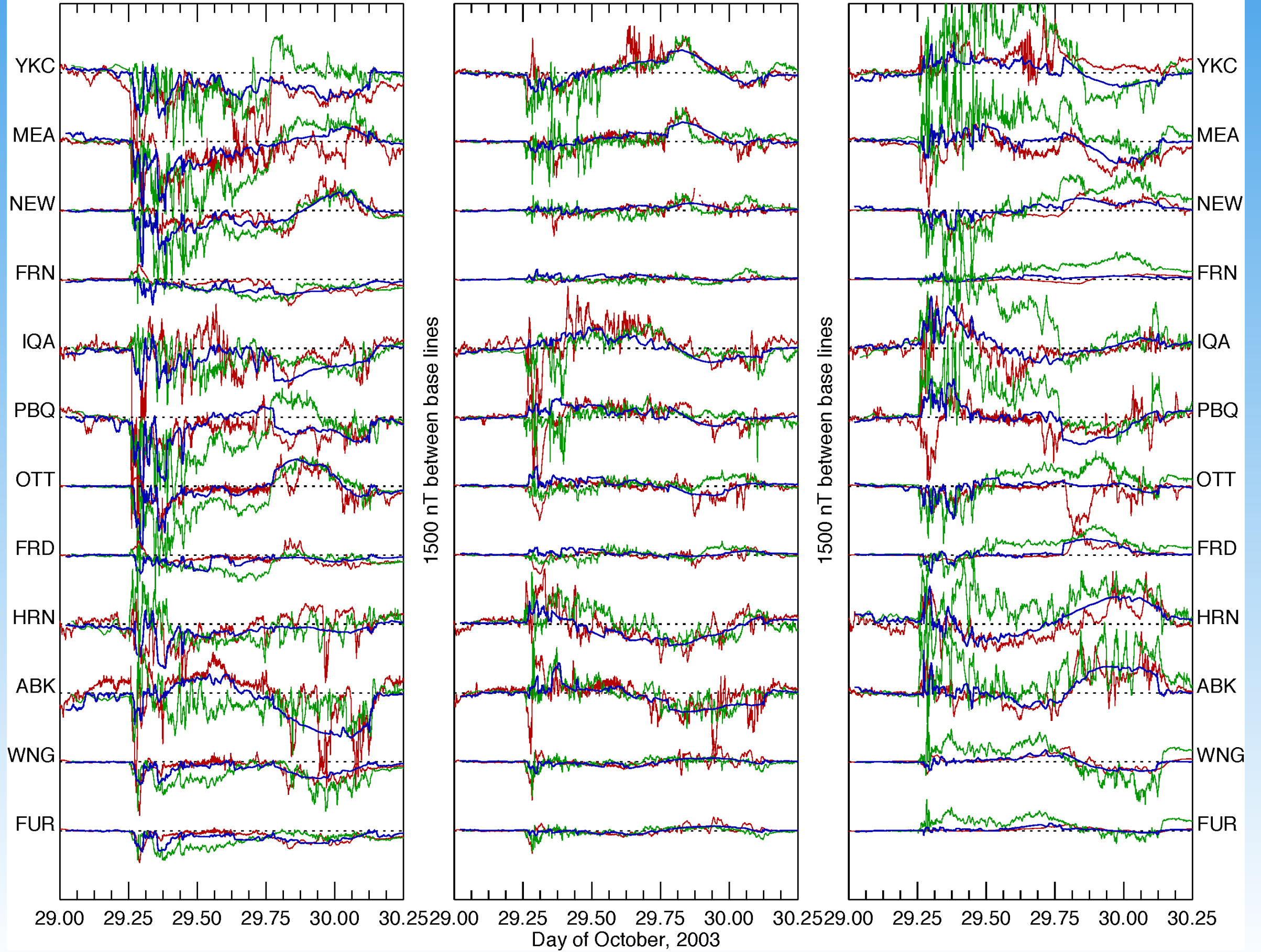
On the other hand, it does not do as well on the more recent tests by CCMC that tested $\delta B/\delta t$ and “Regional-K,” except at mid-latitudes.

These later metrics had used absolute values, and not the signs of ΔB . Data plots on next page show comparison with top MHD model.

BLUE: MODEL 6_WEIMER
North (X)

GREEN: MODEL 9_SWMF
East (Y)

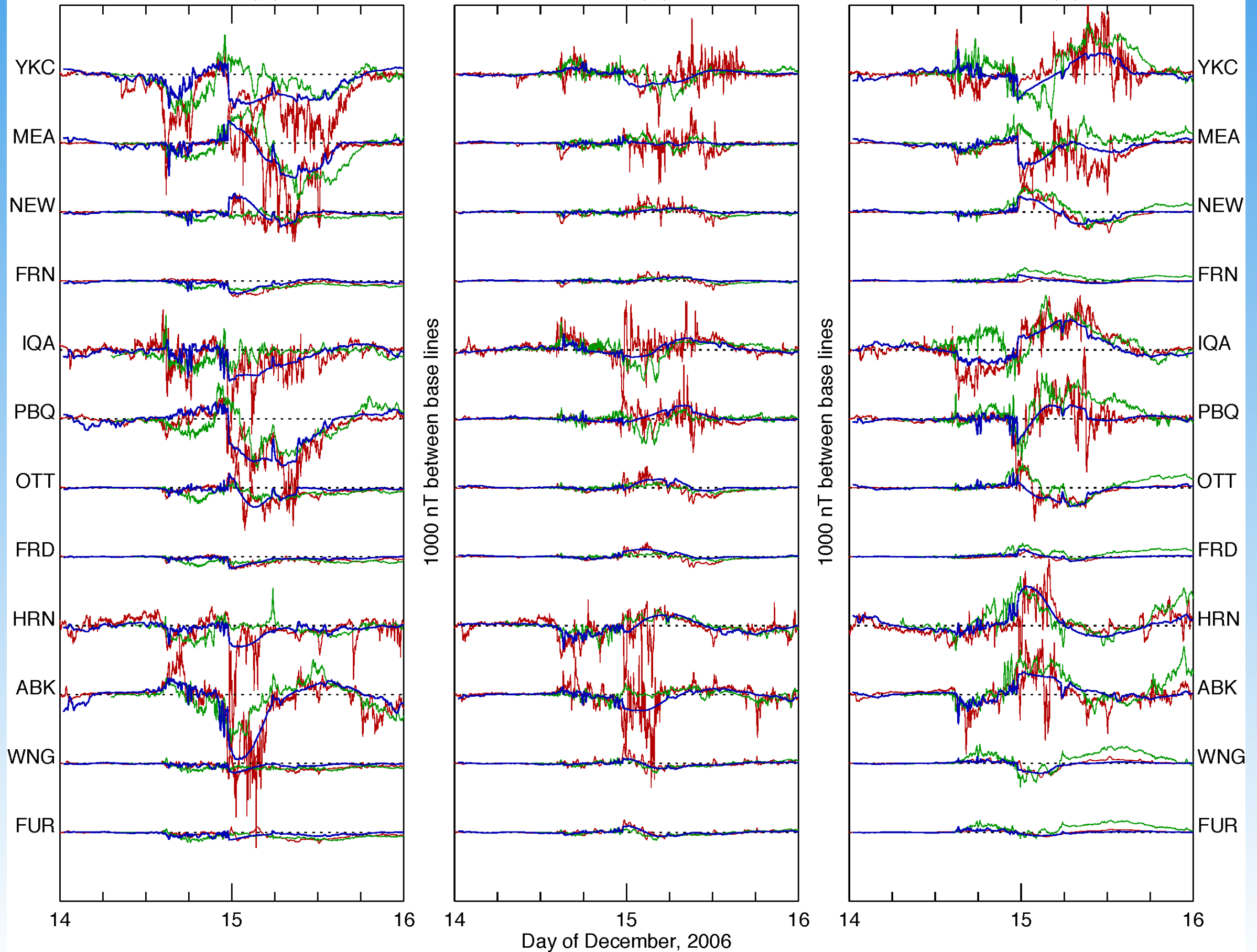
RED: DATA
Vertical (Z)



BLUE: MODEL 6_WEIMER
North (X)

GREEN: MODEL 9_SWMF
East (Y)

RED: DATA
Vertical (Z)

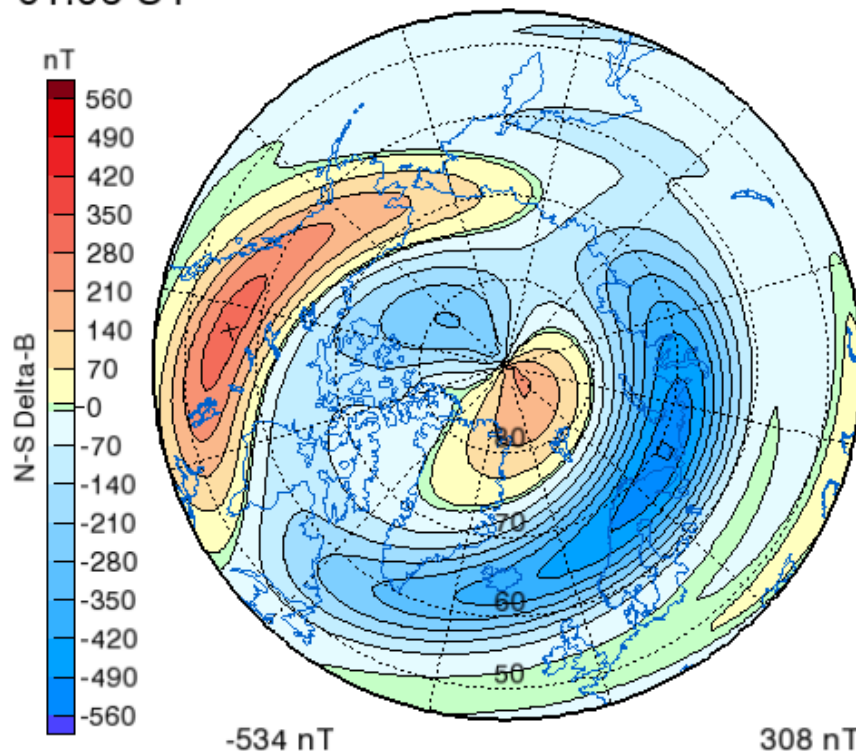


Real-time maps are shown at <http://mist.nianet.org/weimerGeomag.html>
Operating continuously since 2011; plots archived since Sept. 2012



Real-Time Space Weather Predictions Geomagnetic Perturbations at Ground Level

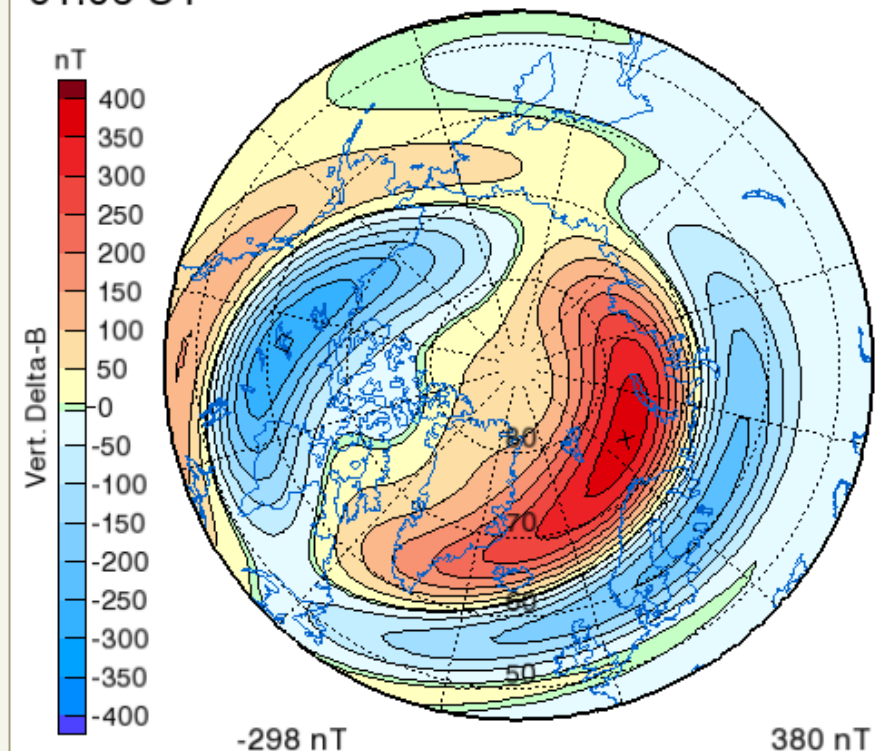
30 April 2011
01:06 UT



North-South Magnetic Perturbations at Surface

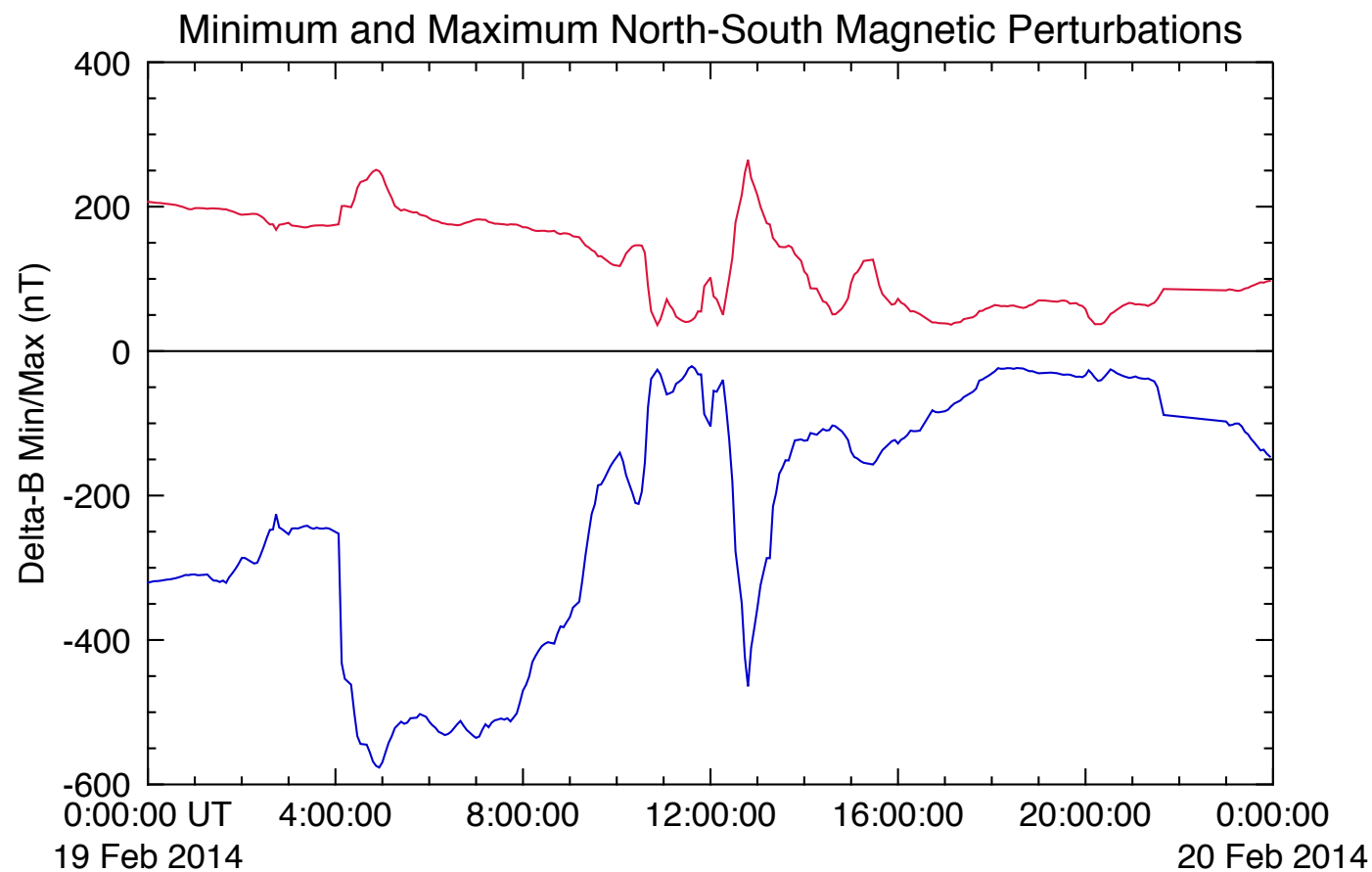
Download PDF file

30 April 2011
01:06 UT



Vertical Magnetic Perturbations at Surface

Download PDF file



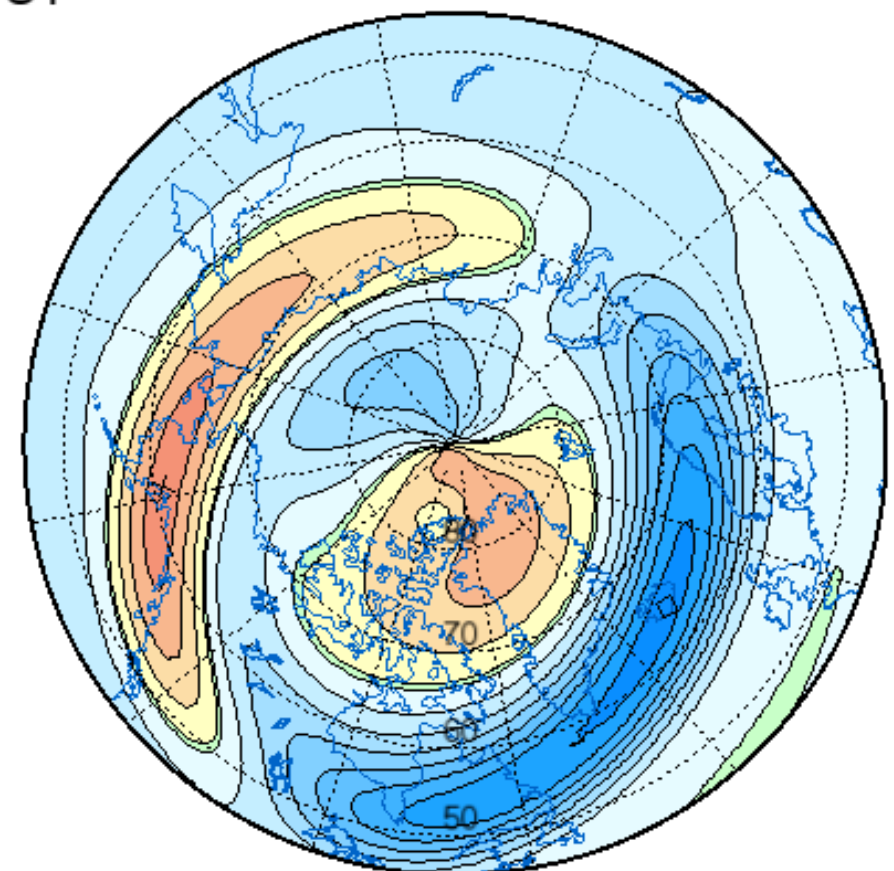
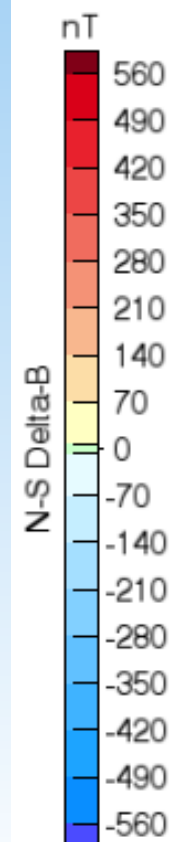
Recent update: Daily summary plots, at <http://mist.nianet.org/weimerDaily.html>

Includes min/max ΔB -North.

Each time step requires \approx five seconds for global-scale calculation, (>32,000 grid points) on an older Mac mini (also used as web server). So it is truly a “rapid, low-cost prediction.”



19 Feb. 2014
04:56 UT

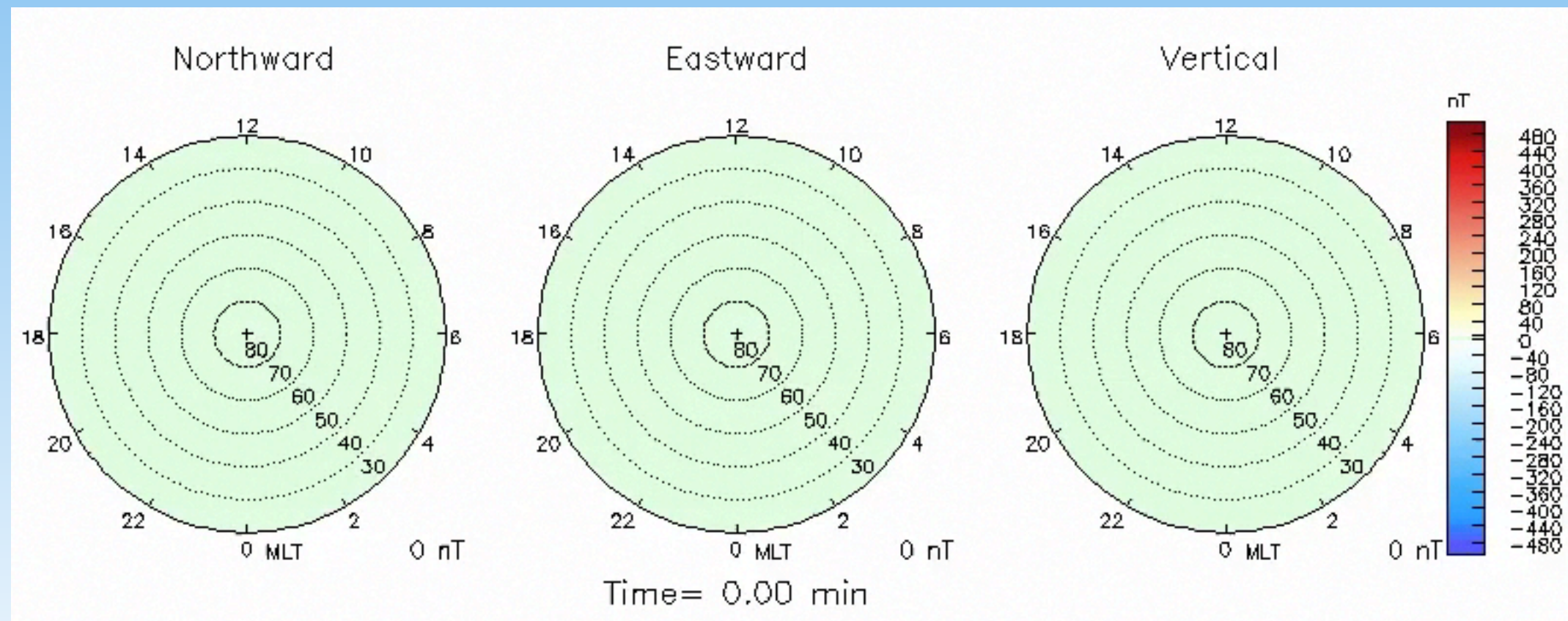


-521 nT

246 nT

Improvements that could be possible in the future:

1. Addition of random “noise” to better predict db/dt thresholds due to chaotic, random turbulence. (Also noted by Toth *et al.*, *JGR*, 119, 310–321, doi:10.1002/2013JA019456, 2014.)
2. Addition of substorm component.



Example of magnetic perturbations during substorms (pre-onset patterns subtracted). $T=0$ is at onset. From Nicole Pothier's M.S. thesis, Hampton University, 2012.

Acknowledgments

The magnetic perturbation prediction was funded by the National Space Weather Program through NSF grant ATM-0817751 to Virginia Tech. The author thanks the many personnel and institutions that maintain the numerous magnetometer arrays:

CARISMA, operated by the University of Alberta, funded by the Canadian Space Agency, the member institutes of INTERMAGNET, the Geophysical Institute of the University of Alaska, Augsburg College MACCS Project, the Danish Meteorological Institute, and the IMAGE Magnetometer Array.

Aurora photo credit: Benjamin Schultz: <http://politesocietymagazine.com/blog/2012/10/day-16-aurora-borealis/>